ACS Catalysis

RESEARCH ARTICLE

pubs.acs.org/acscatalysis

Crystal-Face-Selective Supporting of Gold Nanoparticles on Layered Double Hydroxide as Efficient Catalyst for Epoxidation of Styrene

Fazhi Zhang,* Xiaofei Zhao, Changhong Feng, Bo Li, Tao Chen, Wei Lu, Xiaodong Lei, and Sailong Xu

State Key Laboratory of Chemical Resource Engineering, Beijing University of Chemical Technology, Beijing 100029, China

ABSTRACT: Au catalysts with layered double hydroxide (LDH) as support were fabricated and the crystal faces feature of LDH platelets was revealed to have a crucial effect on the location and particle size of gold nanoparticles (AuNPs). A preferential deposition of AuNPs with a narrow size distribution was formed on the lateral $\{10\bar{1}0\}$ faces of LDH platelets. Catalytic property evaluation of the resulting Au/LDH samples showed that the conversion of styrene with *tert*-butyl hydroperoxide (TBHP) to styrene oxide (SO) occurred on the AuNPs with particle size of 2−3 nm, mainly deposited on the lateral faces of LDH support.

KEYWORDS: Au nanoparticles, layered double hydroxide, crystal face, styrene epoxidation, homogeneous deposition-precipitation

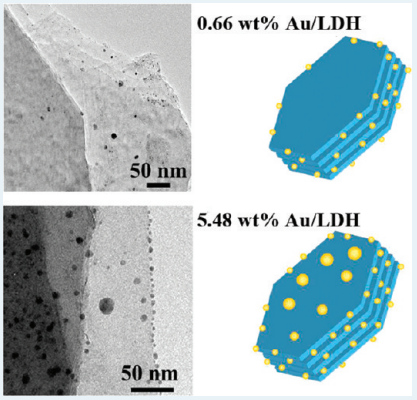

INTRODUCTION

More and more attention of the scientific community has been paid to inorganic nanocrystals with highly reactive surfaces due to their many intrinsic shape-dependent properties, such as optical, electrical, magnetic, and catalytic properties.[1−3] Various previous studies have demonstrated that nanocrystals of metal oxides, such as TiO_2 with a high percentage of {001} faces prepared by using hydrofluoric acid as a capping agent under hydrothermal or water-2-propanol solvothermal conditions, exhibit excellent photocatalytic efficiency.[4,5] Co_3O_4 nanorods with their {110} faces predominantly exposed were reported to exhibit a significantly high reaction rate for low-temperature oxidation of CO[6] and methane combustion.[7] Also, metal nanocrystals, such as tetrahexahedral Pt nanocrystals with high-index faces of {730}, {210}, and {520}, have shown a high catalytic activity for electrooxidation of small organic fuels.[8] Recently, Recently, the crystal-face dependent catalysis by a layered inorganic crystal compound-layered double hydroxide (LDH) has been revealed by Roeffaers et al. who had adapted real time monitoring of the chemical transformation of individual organic molecules by fluorescence microscopy, and they revealed that the activity of base catalysis by LDH, a layered inorganic crystal compound, was dependent on the hydroxyl groups of the types of LDH crystal faces, that is, the ester hydrolysis occurred mainly on the lateral $\{10\bar{1}0\}$ crystal faces, whereas the transesterification took place on the basal {0001} ones.[9] Our recent study has shown that the active sites for the acetone self-condensation maybe the ordered array of hydroxyl groups located mainly on the basal LDH surfaces, rather than on the edges of crystal platelets.[10]

LDH can be expressed by the general formula $[M^{2+}_{1-x}M^{3+}_{x}(OH)_2]^{x+}[A^{n-}]_{x/n}\cdot yH_2O$, where the cations M^{2+} and M^{3+} occupy the octahedral holes in a brucite-like layer and the anion A^{n-} is located in the hydrated interlayer galleries.[11] This flexibility in composition allows LDH with a wide variety of properties to be prepared and is one of their most attractive features. LDH have a wide variety of practical applications including as additives in polymers, as precursors to magnetic materials, and in biology and medicine, catalysis, photochemistry, electrochemistry, and environmental remediation.[12] In particular, LDH represent an interesting opportunity for developing new catalysts, catalyst precursors, and catalyst supports, with tailored structure and properties.[13−15] As a layered material, LDH crystallites tend to have a smooth platelet morphology, in which the dimensions of the (typically hexagonal) basal crystal faces of the platelets are much larger than the thickness (the lateral crystal faces) of the platelets (Figure 1). Since the basal {0001} crystal faces of an LDH, with ordered array of hydroxyl sites on surface, may have a very different electronic structure and energy character from those of the lateral $\{10\bar{1}0\}$ ones with high densities of dangling bonds, the chemical activity of the two types of crystal faces may be expected to show significant differences. Herein, we report the crystal-face-selective supporting of metal nanoparticles on the crystals of LDH.

Gold nanoparticles (AuNPs) have received increasing attention in catalysis since Hutchings[16] and Haruta et al.[17] demonstrated excellent performances of gold-based catalysts in hydrochlorination of acetylene and low temperature oxidation of CO, respectively. The preparation of small AuNPs with narrow size distribution, their stabilization, and their unique properties compared to larger particle size are appealing to a large community of researchers. It is believed that the nature of supports plays an important role in controlling particle size,

Received: November 13, 2010
Revised: January 12, 2011
Published: February 18, 2011

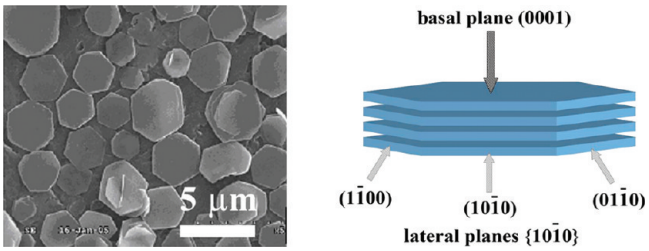

Figure 1. Schematic illustrations of an LDH crystallite with assignment of the different crystal faces.

dispersion level of the particles, and interaction between AuNPs and supports, which can consequentially affect the catalytic performance of the supported AuNPs.[18,19] Thus, it is necessary to selectively utilize the faces of the support to enhance efficiency and stability of AuNPs catalyst.[20−23] In this present study, hexagonal LDH was utilized as support to prepare AuNPs catalyst. Because large crystals with easily identifiable faces are suitable for distinguishing the location of AuNPs in our experiments, an urea decomposition method was adopted for preparation of MgAl-LDH with such crystals in the range of micrometers, by precipitation from homogeneous solution using the temperature-controlled hydrolysis of urea.[24] LDH supported AuNPs catalysts were prepared by a homogeneous deposition−precipitation (HDP) technique using urea as the precursor for precipitating agent.[25] Catalytic performance was evaluated in terms of the conversion of styrene via the epoxidation of styrene with TBHP to SO.

RESULTS AND DISCUSSION

Figure 1 shows a typical scanning electron microscopy (SEM) image of the prepared MgAl-LDH sample. As expected, the MgAl-LDH show flat, well-defined hexagonal basal platelets with fairly large crystal sizes ranging between 1−2 μm. Moreover, as can be seen in Figure 2, MgAl-LDH sample displays the characteristic reflections of the LDH structure with a series of (00l) peaks appearing as narrow, symmetric, and strong lines at low angle. And, the nonbasal reflections (h, $k \neq 0$) at high angle also can be observed for the LDH sample, showing a high crystallinity. Besides, the basal spacing value (d_{003}) of MgAl-LDH is 0.76 nm, which is similar to the values reported in the literature for LDHs with CO_3^{2-} anions in the gallery.[17] The crystallite size in c direction (the stacking direction, perpendicular to the basal layers) can be estimated from the XRD by Scherrer equation [$L = 0.89\lambda/\beta(\theta)\cos\theta$, where L is the crystallite size, λ is the wavelength of the radiation used, θ is the Bragg diffraction angle, and $\beta(\theta)$ is the full width at half-maximum (fwhm) of the (003) and (006) diffraction peaks]. The calculated value is about 23.3 nm. XRD patterns of Au/LDH catalysts with low Au loading (0.10, 0.22 and 0.66%) were found similar to those of the corresponding "pure" LDH, and no diffraction for metallic Au was founded. While with the Au loading increase from 0.66% to 5.48%, the intensity of Au (111) peaks increase gradually.

XPS study was carried out to obtain information on the state of Au in the Au/LDH catalysts. Figure 3 displays the XPS spectra of Au/LDH catalysts containing 0.22, 0.66, 1.93, and 5.48% Au with that of LDH support for comparison. The XPS signal with binding energies near 89.3 and 74.6 eV for all samples is attributed to the Mg 2s and Al 2p, respectively (Figure 3a).

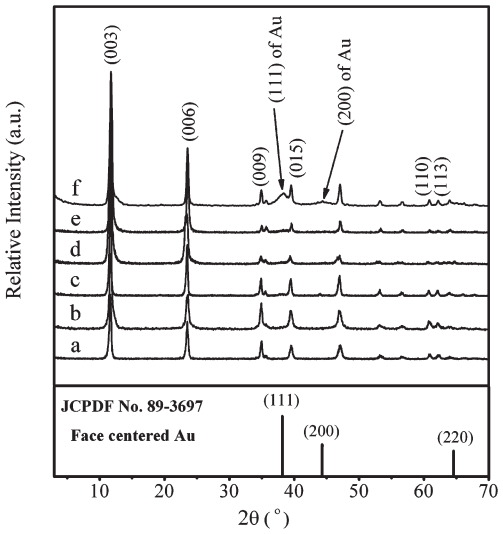

Figure 2. XRD patterns of LDH support (a) and Au/LDH catalysts containing 0.10 (b), 0.22 (c), 0.66 (d), 1.93 (e), and 5.48% Au (f). Pattern of the metal Au phase (JCPDF 89-3697) is included for comparison.

Besides, the four Au/LDH catalysts show two XPS signals of Au 4f near 84.0 and 87.7 eV. According to Park et al.,[26] the XPS data in Figure 3a are characteristic of $4f_{7/2}$ and $4f_{5/2}$ of the metallic Au. Also we can see that the intensity of the two XPS signal of Au 4f enhance with the increase of the Au loading. In addition, the XPS signal located at 335.2 and 353.6 eV represents the Au 4d,[27] whose intensity enhances obviously with the increasing of the Au loading from 0.22% to 5.48% (Figure 3b).

TEM imaging is thought to be the most important experimental technique to establish the particle size distribution and gold dispersion on the support surface. Figure 4 shows the representative transmission electron microscopy (TEM) images of the Au/LDH catalysts with different loading of Au. In the catalyst samples with Au loading of 0.22, and 0.66% (Figure 4a and b), AuNPs are arranged on the lateral {10$\bar{1}$0} crystal faces of LDH support, having average sizes in the range of 2−3 nm. The AuNPs with spherical morphology are highly dispersed without aggregation. Also, quite few AuNPs were found to be on the basal {0001} faces of the LDhH sheets. With the increase of Au loading from 0.66% to 5.48%, the amounts of AuNPs on the basal {0001} faces increase gradually, on which the average sizes of AuNPs are much larger than those on the lateral {10$\bar{1}$0} ones (Table 1). A large amount of AuNPs with particle size exceeding to 10 nm were found on the basal faces for the samples with Au loading of 1.93 and 5.48%.

Previous studies revealed that the solid support of catalyst plays an important role in avoiding particle growth and stabilizing nanoparticles against agglomeration. According to Zanella et al., who developed the HDP method for the preparation of AuNPs supported on TiO_2, the formation of gold surface complexes and colloids gold particles takes place simultaneously.[25] The formation of the surface complex was proposed by reaction of $AuCl_3(OH)^-$ with surface TiOH. Lee and Gavriilidis[28] also suggested a similar mechanism involving the formation of covalent bonds between gold hydroxyl chlorides species in solution and the hydroxyl groups on the surface of alumina. Additionally, the formation of gold colloids was attributed to oxidation−reduction reactions between Au^{3+} and TiO_2 surface, which may reduce

dx.doi.org/10.1021/cs100089v |ACS Catal. 2011, 1, 232–237

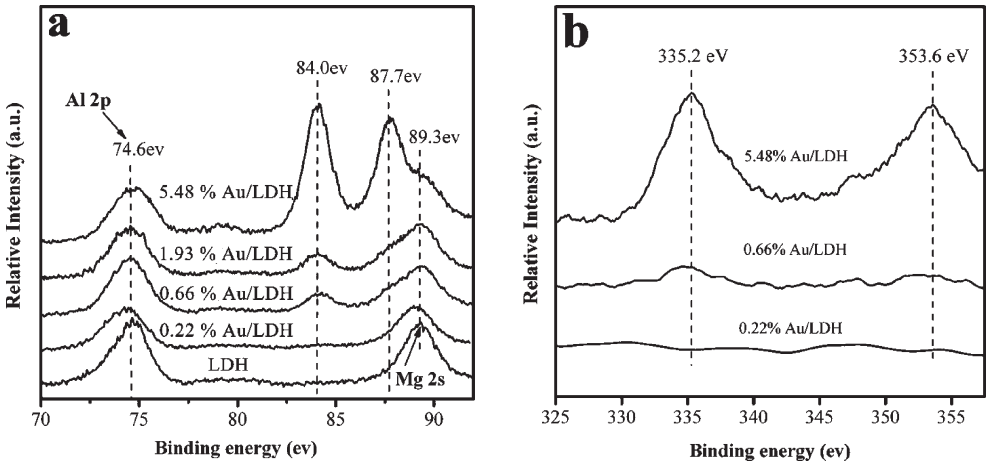

Figure 3. XPS spectra of Au/LDH. Pattern of the MgAl-LDH support is included for comparison.

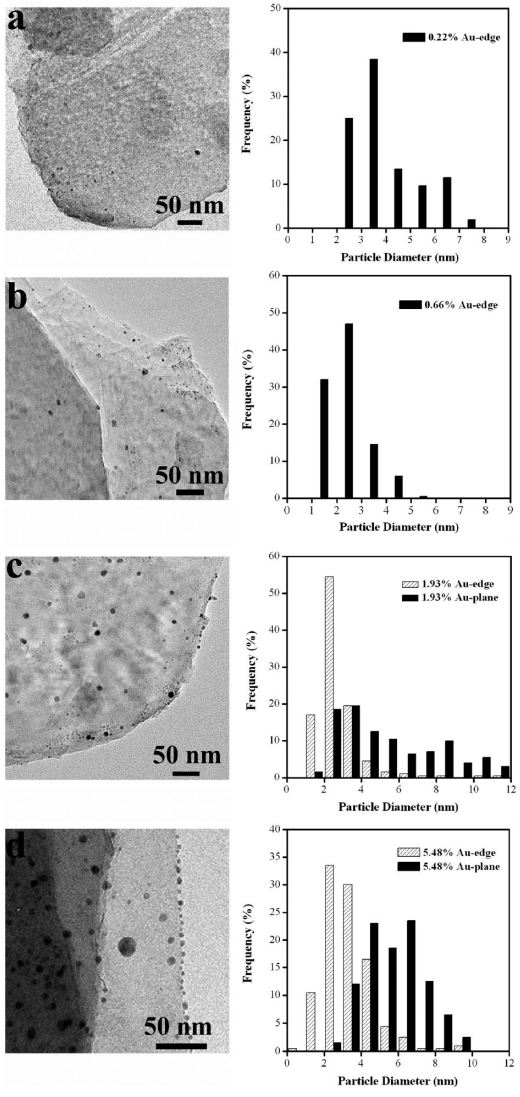

Figure 4. TEM images and the corresponding gold particles distribution of Au/LDH catalysts containing 0.22 (a), 0.66 (b), 1.93 (c), and 5.48% Au (d).

gold because it usually contains defects of Ti^{3+} ions. Adsorption of gold on the oxidizable mineral surfaces initially induces the

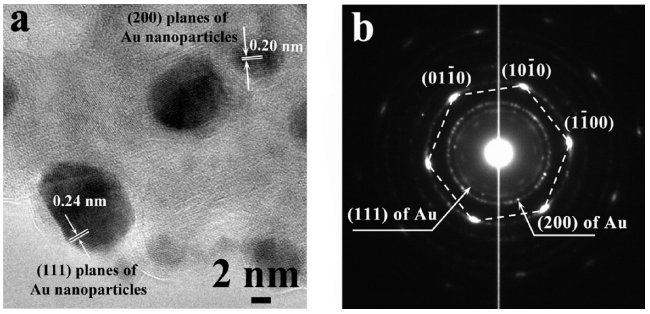

Figure 5. HRTEM image (a) and the corresponding selected area electron diffraction pattern (b) of Au/LDH catalyst containing 1.93% Au.

reduction of Au^{3+} to elemental gold, which is subsequently sorbed on the oxide support. The colloidal gold particles are indeed negatively surface-charged,[29] so the particles can react with positively charged TiO_2 by electrostatic interaction under the preparation conditions. Thus, it is rational to hypothesize that the interaction between Au species and support is crucial for the deposition of AuNPs. It is well-known that the structure of LDH is based on brucite ($Mg(OH)_2$)-like layers in which some of the divalent cations have been replaced by trivalent ions giving positively charged sheets.[12] So, the surface feature of LDH is beneficial to interact with the gold surface complexes and colloids. In addition, the atoms on the lateral face of a LDH crystal facet are incompletely bonded within the crystal lattice, thus disrupting the crystalline periodicity and leaving one or more "dangling orbital" on each atom pointed outward from the crystal. The lateral $\{10\bar{1}0\}$ faces with high densities of dangling bonds, may have a relatively active chemical characteristic, resulting in the preferential deposition of AuNPs on the $\{10\bar{1}0\}$ face with the increase of Au loading. The strong interaction between the lateral $\{10\bar{1}0\}$ crystal faces and the AuNPs can prevent the aggregation of particles under the air calcination at 473 K, signifying that the particle size of AuNPs on the lateral faces is much smaller than those on the basal ones for the two samples in the case of the Au loading of 1.93 and 5.48%. More detailed structural information about the AuNPs deposited on the LDH support can be obtained from HRTEM and the corresponding selected area electron diffraction (SAED) pattern.

dx.doi.org/10.1021/cs100089v |*ACS Catal.* 2011, 1, 232–237

Table 1. Average Au particle size (TEM) and Reaction Results of Epoxidation of Styrene with TBHP over Au/LDH Catalysts[a]

		d_{Au} (nm)[c]			selectivity (%)						
catalyst[b]	Au loading (wt %)	on lateral {10$\bar{1}$0} face	on basal {0001} face	styrene conv. (%)	SO	BD	PA	TBHP conv. (%)	yield of SO (%)	TOF[c] (h^{-1})	ref.
LDH				6.8	73.7	21.2	5.3	11.1	5.0		this work
Au/LDH	0.10			41.8	89.1	8.6	2.4	36.6	37.3	970.2	this work
Au/LDH	0.22	3.9 ± 1.3		63.0	81.7	15.6	2.7	56.6	51.5	479.1	this work
Au/LDH	0.66	2.5 ± 0.8		67.4	73.5	21.3	5.2	64.2	49.5	157.2	this work
Au/LDH	1.93	2.9 ± 1.3	5.6 ± 2.8	56.1	74.8	23.1	2.1	59.1	41.9	53.8	this work
Au/LDH	5.48	3.4 ± 1.4	5.8 ± 1.5	79.4	74.2	24.3	1.5	88.4	58.9	26.5	this work
Au/MgO	7.5	7.9 ± 0.3		62.6	54.3	10.8	16.8		34.0	29.8	32, Table 1, Fiugre 2
Au/Al_2O_3	6.36	4.1 ± 2.3		~44	~28	~24	~13	~100	~12.3	~11.4	33, Table 1, Figure 3
Au/TiO_2	6.00	2.8 ± 0.8		~61	~53	~10	~17		~32.3	~34.4	34, Table 1, Figure 3
Au/*meso*-Al_2O_3	2.0			84.3	69.0	23.0	3.6		58.2	47.8	35, Table 2, Figure 3
meso-Al_2O_3				50.3	66.9	21.0	5.2		33.7		35, Table 2
Au/HAP	0.5	1.4 ± 0.6		100.0	92.0				92.0	114.0	36

[a] Reaction conditions: catalyst, 0.1 g; temperature, 353 K; time, 8 h; styrene, 10.18 mmol (1.17 mL); TBHP, 28.58 mmol (2.8 mL); benzene, 56.24 mmol (5 mL). SO: styrene oxide. BD: benzaldehyde. PA: phenyl acetaldehyde. [b] All catalyst samples were prepared by HDP. [c] The average particle size of Au was determined according to the equation $d = \Sigma n_i d_i / n_i$ by randomly measuring for each sample ~500 particles by TEM. The standard deviation was calculated from the formula $\sigma = [(\Sigma(d_i - d)^2)/\Sigma n_i]^{1/2}$.

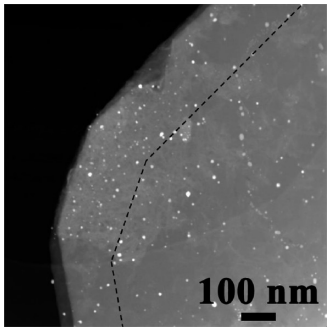

Figure 6. Representitive STEM-HAADF images of the 0.66 wt % Au/LDH catalyst.

As can be seen in Figure 5a, the spacing of the crystallographic planes of 0.24 and 0.20 nm agrees well with the (111) and (200) lattice planes of the AuNPs, and supports the polycrystalline nature of those AuNPs. The SAED pattern (Figure 5b) shows the standard face-centered structure of such polycrystalline AuNPs and the diffraction rings corresponding to the (111) and (200) planes can be observed clearly. Moreover, the hexagonal appearance in such SAED pattern corresponds to the {10$\bar{1}$0} crystalline planes of the high-crystallined LDH supports. Aberration-corrected STEM-HAADF imaging was utilized to further determine the size distribution of AuNPs supported on the MgAl-LDH. As shown in Figure 6, obvious different particle size distribution of AuNPs on lateral/basal planes (outside/inside the dotted line) of LDHs can be observed.

Catalytic activity of the Au/LDH catalysts is shown in Table 1 for the epoxidation of styrene with TBHP as oxidant to SO. The pure LDH exhibited an appreciable selectivity of 73.7% for SO but with a very low reaction activity (styrene conversion of 6.8% and TBHP conversion of 11.1%). Upon loading AuNPs, the resulting Au/LDH showed a rapid increase in the reactant conversion. Table 1 shows that the styrene conversion first increased from 41.8% to 67.4% as the Au loading rose from 0.10% to 0.66%, and then underwent a decrease with an increase in Au loading to 1.93%. Further increases in Au loading, however, caused the increases in styrene conversion again. Also, we can see that the TBHP conversion showed the same trend within the experimental range. Although the size of AuNPs alone does not seem to be a sufficient factor for the high activity of nanosized Au catalysts, the exploration of the catalytic performance of AuNPs on the reduce of the size has been the main focus of most research in this field.[18,19] Haruta et al.[30] reported that the catalytic activity of Au catalyst on different oxide supports (TiO_2, α-Fe_2O_3, Co_3O_4) increases with the decreasing of the particle size of AuNPs in the range of 2−10 nm. Valden et al.[31] found that AuNPs of about 3.5 nm showed the highest activity in a series of Au/TiO_2 catalysts. Table 1 demonstrates that the Au/LDH with Au loading of 1.93% showed neither a higher styrene conversion nor an enhanced SO yield in comparison with Au loading of 0.66%. Figure 4c shows that the Au/LDH sample with Au loading of 1.93% contained a large percentage of AuNPs with particle size larger than 10 nm located on the basal faces. Previous studies have demonstrated that catalytic activity of AuNPs is directly related to particle size at the nanometer scale. The catalytic activity of AuNPs is found to decrease rapidly as the particle size grows beyond 10 nm. In our case, we thus propose that the conversion of styrene for the Au/LDH catalyst may be conducted on the AuNPs with particle size of 2−3 nm, which were deposited on the lateral {10$\bar{1}$0} crystal faces of the LDH support. The turnover of frequency (TOF) values of series of Au/LDH catalysts have been calculated. As can be seen in Table 1, when the loading of Au is 0.1 wt %, the TOF value reaches 970.2 h^{-1}; with the increasing of the Au loading, the TOF value decreases obviously, when the loading of Au is 5.48 wt %, the TOF value is only 26.5 h^{-1}. The variation trend of TOF value also confirms the catalytic reaction are closely associated with the AuNPs located on the {10$\bar{1}$0} lateral crystal faces of LDH support. Meanwhile, with the increasing loading of Au on the LDH, the selectivity of SO showed a declining trend: with Au loading ranging from 0.10% to 0.66%, the selectivity of SO decreased from 89.1% to 73.5%. The main side-production is benzaldehyde, with trace phenyl acetaldehyde. With the Au

dx.doi.org/10.1021/cs100089v |ACS Catal. 2011, 1, 232–237

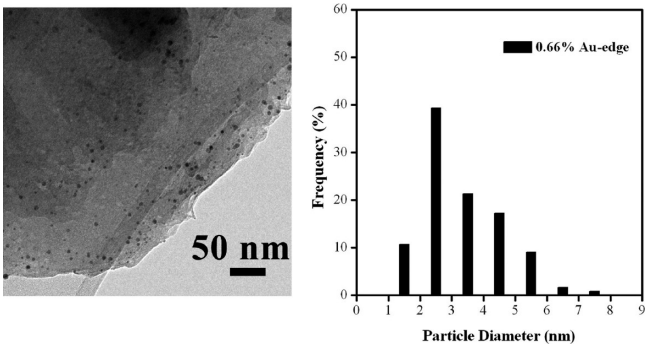

Figure 7. TEM image and the corresponding particle distribution of the used Au/LDH catalyst containing 0.66% Au.

loading further increase, the catalyst samples can keep the similar selectivity of SO. Figure 7 shows the TEM image and the corresponding particle size distribution of the used Au/LDH with Au loading of 0.66%. The preferential deposition of AuNPs has been well preserved during/after the course of reaction, and the particle size of the AuNPs on the lateral $\{10\bar{1}0\}$ face is 3.0 ± 0.7 nm, which is very similar to that of the sample before the reaction. Such results indicate that the Au/LDH catalysts show well structural stability after the epoxidation reaction.

A comprehensive evaluation of our Au/LDH catalyst with other reported Au catalysts under the similar reaction condition has been done, as can be seen in Table 1. Compared to the metal oxide-supported Au/MgO,[34] Au/Al_2O_3,[33] and Au/TiO_2[34] catalysts with Au loading larger than 6 wt %, our 5.48 wt % Au/LDH catalyst displays an enhanced conversion of styrene and TBHP and SO selectivity. Although a mesoporous alumina-supported Au/*meso*-Al_2O_3 catalyst showed 84.3% of styrene conversion, the high conversion of styrene was attributed predominately to contribution from the mesoporous alumina support.[35] Recently, Au_{25} clusters supported on hydroxyapatite was developed by Liu et al.,[36] which oxidized styrene in toluene with 100% conversion and 92% selectivity to the epoxide, under optimum conditions.

To check if the catalyst retained its original activity and selectivity, 0.1 g of catalyst (0.66% wt% Au/LDH) was repeatedly used for the epoxidation of styrene for three times, and the experimental results are plotted in Figure 8, overlaid with the results obtained for fresh catalyst. The results show excellent reusability with an evident improvement in both catalytic activity and selectivity in the epoxidation.

In summary, we have demonstrated the preferential deposition of AuNPs with a narrow size distribution on the lateral $\{10\bar{1}0\}$ faces of LDH platelets. The crystal-face-selective supporting of AuNPs on the LDH support can efficiently catalyze the epoxidation of styrene with TBHP as oxidant to the SO production. The conversion of styrene may occur on the AuNPs with particle size of 2−3 nm, mainly deposited on the lateral faces of LDH support. Our results show that the general formulation of our experimental regulation, that depositing is controlled by preferential adsorption on the highly reactive surface, provides a framework appropriate for other layered inorganic crystal compound and noble metal nanoparticles as well.

EXPERIMENTAL SECTION

Preparation of MgAl-LDH Support. A solution of $Mg(NO_3)_2 \cdot 6H_2O$ and $Al(NO_3)_3 \cdot 9H_2O$ dissolved in 75 mL of deionized water with Mg^{2+}/Al^{3+} molar ratio of 2.0 and a total

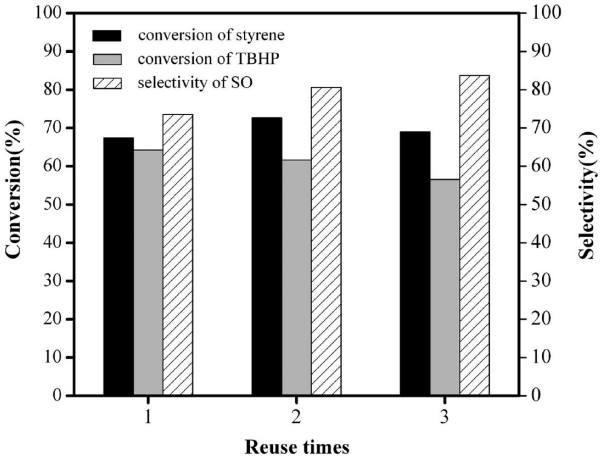

Figure 8. Reuse results of the 0.66 wt % Au/LDH: the conversion of styrene and TBHP, and the selectivity of SO.

concentration of metal cations of 0.3 M, was placed in a polytetrafluoroethylene vessel. Urea ($[urea]/[NO_3^-]$ = 4.0) was dissolved in the above solution. The container was sealed and placed in an oven and maintained at 363 K for 3 days. The solid was collected by filtration, washed with deionized water until the washings reached a pH of 7.0, and subsequently dried at 373 K for 24 h.

Preparation of LDH-Supported AuNPs Catalysts. LDH supported AuNPs catalysts were prepared by the homogeneous deposition−precipitation (HDP) using urea as the precursor for precipitating agent.[20] In a typical procedure, a known amount of hydrogen tetrachloroaurate (III) trihydrate ($HAuCl_4 \cdot 3H_2O$, purchased from J&K Chemical Ltd.) with appropriate concentrations, which was adjusted to yield catalysts containing 0.10, 0.22, 0.66, 1.93, and 5.48 wt % Au, was prepared advanced and stored at room temperature. Urea was added to the $HAuCl_4$ solution to achieve a concentration of 0.42 M to a 100 mL round-bottom flask, and then LDH powders were dispersed in the $HAuCl_4$ solution. This aqueous dispersion was under continuous stirring for 5 h at the temperature of 353 K and then aged for 2 h. After the mixture was filtered, extensive washing with deionized water then followed until it was free of chloride ions. Vacuum drying at 363 K and air calcination at 473 K for 5 h of the sample finalized the preparation of Au/LDH catalysts.

Characterization. Powder X-ray diffraction (XRD) patterns were collected on a Shimadzu XRD-6000 instrument with Cu Kα radiation in the 2θ range from 3° to 70°. Elemental analyses for Au were performed by inductively coupled plasma emission spectrometry (ICP-ES) using a Shimadzu ICP-7500 instrument. Samples were dried at 100 °C for 24 h prior to analysis, and solutions were prepared by dissolving the samples in dilute hydrochloric acid. To determine the Cl^- ions on the Au/LDH catalysts, different samples with Au loading of 0.10 wt %, 0.22 wt %, 0.66 wt %, and 1.93% were selected and characterized by X-ray Fluorescence Spectrometer (XRF) on Bruker AXS S4-Explorer. No signal of Cl^- is detected for samples with Au loading of 0.10 wt %, 0.22 and 0.66 wt %, because the amount of Cl^- ions on the LDH is lower than the detection limit 100 ppm. While for the 1.93 wt % Au/LDH sample, the residual Cl^- is only 350 ppm. Therefore, it is concluded that the residual Cl^- ions of as-prepared Au/LDH catalysts can be negligible. Transmission electron micrographs (TEM) analyses were performed on Tecnai G^2 F20 UTWIN (200 kV); scanning transmission

dx.doi.org/10.1021/cs100089v |*ACS Catal.* 2011, 1, 232–237

electron microscopy and high-angle annular dark-field (STEM-HAADF) imaging was carried out to determine the particle size distribution in the catalyst. Scanning electron microscopy (SEM) was recorded on a Zeiss Supra 55 instrument. X-ray photoelectron spectra (XPS) of the catalysts were recorded with an SKL-12 spectrometer equipped with Mg Kα radiation. The binding energies of Au 4f were corrected for surface charging by referencing them to the energy of C 1s peak of contaminant carbon at 285.0 eV. The catalytic reaction was monitored by a gas chromatography (Shimadzu Technologies, HP-624 capillary column, 30 m × 0.25 mm) with flame ionization detector using nitrogen as carrier gas and tetradecane as an internal standard substance. Both the injector and detector temperature were 523 K. The products were identified by GC−MS using an HP5790 series mass selective detector. The reactant conversion, product selectivity and styrene oxide (SO) yield were calculated as follows: reactant conversion (%) = [(moles of reactant converted) × 100]/[(moles of reactant in feed)], product selectivity (%) = [(moles of product formed) × ·100]/[(moles of reactant converted)], and SO yield (%) = [reactant styrene conversion (%) × product SO selectivity (%)/100].

Catalytic Reaction Procedure. The styrene epoxidation reaction over the supported Au catalysts were carried out under air by contacting 0.1 g of the catalyst with 10.18 mmol of styrene (1.17 mL), 28.58 mmol (2.8 mL) of aqueous TBHP (65 wt.% in water) and 56.24 mmol (5 mL) of benzene in a magnetically stirred glass reactor at the temperature of 353 K for 8 h. The 0.66 wt % Au/LDH catalyst was selected for repeating the epoxidation process for 3 times. The catalysts were recovered by filtration, washed with acetone, and then dried overnight at 313 K for 24 h under vacuum conditions. Then the recovered powder 0.1 g was used to perform a new reaction of epoxidation under the previous conditions.

Recyclability of 0.66 wt % Au/LDH Catalyst. The 0.66 wt % Au/LDH catalyst was selected for repeating the epoxidation process for 3 times. The catalysts were recovered by filtration, washed with acetone, and then dried overnight at 313 K for 24 h under vacuum conditions. Then the recovered powder 0.1 g was used to perform a new reaction of epoxidation under the previous conditions.

AUTHOR INFORMATION

Corresponding Author

*Tel: (+86) 10-6442-5105. Fax: (+86) 10-6442-5385. E-mail: zhangfz@mail.buct.edu.cn.

ACKNOWLEDGMENT

This work was financially supported by the National Natural Science Foundation of China, the 973 Program (No. 2009CB939802), the Program for New Century Excellent Talents in Universities (No. NCET-07-0055), and the Fundamental Research Funds for the Central Universities (No. ZZ0916).

REFERENCES

(1) Yin, Y. D.; Alivisatos, A. P. *Nature* **2005**, *437*, 664–670.
(2) Sun, Y. G.; Xia, Y. N. *Science* **2002**, *298*, 2176–2179.
(3) Peng, X. G.; Manna, L.; Yang, W. D.; Wickham, J.; Scher, E.; Kadavanich, A.; Alivisatos, A. P. *Nature* **2002**, *404*, 59–61.
(4) Yang, H. G.; Sun, C. H.; Qiao, S. Z.; Zou, J.; Liu, G.; Smith, S. C.; Cheng, H. M.; Lu, G. Q. *Nature* **2008**, *453*, 638–642.
(5) Han, X. G.; Kuang, Q.; Jin, M. S.; Xie, Z. X.; Zheng, L. S. *J. Am. Chem. Soc.* **2009**, *131*, 3152–3153.
(6) Xie, X. W.; Li, Y.; Liu, Z. Q.; Haruta, M.; Shen, W. J. *Nature* **2009**, *458*, 746–749.
(7) Hu, L. H.; Peng, Q.; Li, Y. D. *J. Am. Chem. Soc.* **2008**, *130*, 16136–16137.
(8) Tian, N.; Zhou, Z. Y.; Sun, S. G.; Ding, D.; Wang, Z. L. *Science* **2007**, *316*, 732–735.
(9) Roeffaers, M. B. J.; Sels, B. F.; Uji-i, H.; De Schryver, F. C.; Jacobs, P. A.; De Vos, D. E.; Hofkens, J. *Nature* **2006**, *439*, 572–575.
(10) Lei, X. D.; Zhang, F. Z.; Yang, L.; Guo, X. X.; Tian, Y. Y.; Fu, S. S.; Li, F.; Evans, D. G.; Duan, X. *AIChE J.* **2007**, *53*, 932–940.
(11) Auerbach, S. M.; Carrado, K. A. In *Handbook of Layered Materials*, 1st ed.; Dutta, P. K. Eds.; M. Dekker, Inc., New York, 2004; Vol 1, p 1.
(12) Li, F.; Duan, X. *Struct. Bonding (Berlin)* **2006**, *119*, 193–223.
(13) Cavani, F.; Trifiró, F.; Vaccari, A. *Catal. Today* **1991**, *11*, 173–301.
(14) Vaccari, A. *Appl. Clay Sci.* **1991**, *14*, 161–198.
(15) Tichit, D.; Coq, B. *Cattech* **2003**, *7*, 206–217.
(16) Hutchings, G. J. *J. Catal.* **1985**, *96*, 292–295.
(17) Haruta, M.; Kobayashi, T.; Sano, H.; Yamada, N. *Chem. Lett.* **1987**, *16*, 405–408.
(18) Corma, A.; Garcia, H. *Chem. Soc. Rev.* **2008**, *37*, 2096–2126.
(19) Daniel, M. C.; Astruc, D. *Chem. Rev.* **2004**, *104*, 293–346.
(20) Pietron, J. J.; Stroud, R. M.; Rolison, D. R. *Nano Lett.* **2002**, *2*, 545–549.
(21) Bollinger, M. A.; Vannice, M. A. *Appl. Catal., B* **1996**, *8*, 417–443.
(22) Zheng, N. F.; Stucky, G. D. *J. Am. Chem. Soc.* **2006**, *28*, 14278–14280.
(23) Chen, L. F.; Hu, J. C; Richards, R. *J. Am. Chem. Soc.* **2009**, *131*, 914–915.
(24) Adachi-Pagano, M.; Forano, C.; Besse, J.-P. *J. Mater. Chem.* **2003**, *13*, 1988–1993.
(25) Zanella, R.; Giorgio, S.; Henry, C. R.; Louis, C. *J. Phys. Chem. B* **2002**, *106*, 7634–7642.
(26) Park, E. D.; Lee, J. S. *J. Catal.* **1999**, *186*, 1–11.
(27) Enache, D. I.; Edwards, J. K.; Landon, P.; Solsona-Espriu, B.; Carley, A. F.; Herzing, A. A.; Watanabe, M.; Kiely, C. J.; Knight, D. W.; Hutching, G. J. *Science* **2006**, *311*, 362–365.
(28) Lee, S. J.; Gavriilidis, A. *J. Catal.* **2002**, *206*, 305–313.
(29) Enzweiler, J.; Joekes, I. *J. Geochem. Explor.* **1991**, *40*, 133–142.
(30) Haruta, M.; Tsubota, S.; Kobayashi, T.; Kageyama, H.; Genet, M. J.; Delmon, B. *J. Catal.* **1993**, *144*, 175–192.
(31) Valden, M.; Lai, X.; Goodman, D. W. *Science* **1998**, *281*, 1647–1650.
(32) Patil, N. S.; Uphade, B. S.; Jana, P.; Bharagava, S. K.; Choudhary, V. R. *J. Catal.* **2004**, *223*, 236–239.
(33) Patil, N. S.; Jha, R.; Uphade, B. S.; Bhargava, S. K.; Choudhary, V. R. *Appl. Catal., A* **2004**, *275*, 87–93.
(34) Patil, N. S.; Uphade, B. S.; McCulloh, D. G.; Bhargava, S. K.; Choudhary, V. R. *Catal. Commun.* **2004**, *5*, 681–685.
(35) Yin, D. H.; Qin, L. S.; Liu, J. F.; Li, C. Y.; Jin, Y. *J. Mol. Catal. A: Chem.* **2005**, *240*, 40–48.
(36) Liu, Y. M.; Tsunoyama, H.; Akita, T.; Tsukuda, T. *Chem. Commun.* **2010**, *46*, 550–552.